

Dynamic Properties of Outwardly Propagating Spherical Hydrogen–Air Flames at High Temperatures and Pressures

Oh Chae Kwon*

*School of Mechanical Engineering, Sungkyunkwan University,
300 Chunchun-dong, Jangan-gu, Suwon, Kyunggi-do 440-746, Korea*

Computational experiments on fundamental unstretched laminar burning velocities and flame response to stretch (represented by the Markstein number) of hydrogen–air flames at high temperatures and pressures were conducted in order to understand the dynamics of the flames including hydrogen as an attractive energy carrier in conditions encountered in practical applications such as internal combustion engines. Outwardly propagating spherical premixed flames were considered for a fuel–equivalence ratio of 0.6, pressures of 5 to 50 atm, and temperatures of 298 to 1000 K. For these conditions, ratios of unstretched–to–stretched laminar burning velocities varied linearly with flame stretch (represented by the Karlovitz number), similar to the flames at normal temperature and normal to moderately elevated pressures, implying that the “local conditions” hypothesis can be extended to the practical conditions. Increasing temperatures tended to reduce tendencies toward preferential–diffusion instability behavior (increasing the Markstein number) whereas increasing pressures tended to increase tendencies toward preferential–diffusion instability behavior (decreasing the Markstein number).

Key Words : Hydrogen Flames, High Temperature and Pressure, Markstein Numbers, Laminar Burning Velocities, Preferential Diffusion, Stretch

1. Introduction

Hydrogen is an attractive energy carrier, which can be used as a fuel in combustion of hydrogen–air mixtures for the applications such as auto– and aero–propulsion systems, or as an energy source without combustion for the applications such as fuel cells. The burning of hydrogen–air mixtures offers the potential of reduced pollutant formation and improvement in performance due to the wide flammability limits and the high flame propagation speeds, compared to the burning of traditional hydrocarbon–air mixtures

(DeLuchi, 1989 ; Poulton, 1994). In addition, hydrogen is preferred to methanol or hydrocarbons for fuel cells due to a simpler design with direct hydrogen storage onboard vehicles (Ogden, 1999). Thus there have been various studies on hydrogen combustion and hydrogen economy (DeLuchi, 1989 ; Mathur et al., 1992 ; Ogden, 1999 ; Verhelst and Sierens, 2001).

While those studies demonstrated that hydrogen could be advantageously used as a fuel in the near future, there exist some concerns about directly using pure hydrogen : e.g. the problems of storage and safety and the technical problems such as engine knocking. In order to avoid such the possible problems of using pure hydrogen as a fuel, more efforts have been made to use hydrogen in a somewhat passive way, e.g. as an additive to hydrocarbon fuels. Recently, there have been considerable studies on the feasibility of such the hydrogen use (Kyaw and Watson, 1992 ;

* E-mail : okwon@skku.edu

TEL : +82 31-290-7465; FAX : +82 31-290-5849

School of Mechanical Engineering, Sungkyunkwan University, 300 Chunchun-dong, Jangan-gu, Suwon, Kyunggi-do 440-746, Korea. (Manuscript Received August 13, 2003; Revised November 21, 2003)

Bell and Gupta, 1997) and the related fundamental studies on the burning of hydrogen-added hydrocarbon-air mixtures (Yu et al., 1986; Yamaoka and Tsuji, 1992; Gauducheau et al., 1998).

Although the use of hydrogen as an additive to the traditional hydrocarbon-air mixtures obviously improves the performance in applications, it is not enough considering recent and future higher pollution standards: more direct use of hydrogen is expected in the near future. Thus, the expected extensive use of hydrogen in the near future requires for more understanding of the fundamental dynamics of the hydrogen-air flames.

It is widely recognized that flame/stretch interactions, due to preferential diffusion of various species and heat, can significantly affect the propagation velocities and structure of premixed flames (Markstein, 1964; Strehlow and Savage, 1978; Clavin, 1985; Law, 1988; Dowdy et al., 1990; Bradley et al., 1998; Sun et al., 1999), including laminar premixed hydrogen-fueled flames (Aung et al., 1998; Kwon and Faeth, 2001) and strongly turbulent premixed hydrogen-fueled flames typical of practical applications (Aung et al., 2002). However, the previous studies of flame/stretch interactions for the hydrogen-fueled flames are limited to combustion at normal temperature and normal to moderately elevated pressures although conditions encountered in practical applications such as internal combustion engines are of high temperatures and pressures. Thus, the objective of the present investigation was to consider effects of pressure and temperature variations to understand the dynamics of the flames including such the attractive energy carrier in the practical conditions with the following specific objectives. The first is to numerically measure the burning velocity/stretch interactions of the outwardly propagating hydrogen-air flames at high temperatures and pressures, and thereby to explore a linear correlation between the burning velocities and stretch based on the "local conditions" hypothesis of Kwon et al. (1992), which will be discussed in the next section. The second is to extract the laminar burning

velocities from the flame/stretch interaction data, based on the "local conditions" hypothesis. The third is to measure Markstein numbers (representing the sensitivities of flame response to stretch, and related to the flame surface instabilities) to understand the dynamic behavior of the flames.

The results for the burning velocity/stretch interactions, the Markstein numbers and the laminar burning velocities will be subsequently discussed, following the discussion of the computational methods used during the present investigation in the next section.

2. Computational Methods

The outwardly propagating spherical flame was adopted as the model flame for the present investigation. Fundamentally, the flame is relatively easy to generate and its global configuration and dynamics are also well defined. Practically, it is the phenomenon that is most relevant to combustion in the spark ignition engines and accidental explosions (Kwon et al., 2002).

The outwardly propagating spherical laminar premixed flames were simulated using the algorithm for the unsteady one-dimensional laminar flame (RUN-1DL), developed by Rogg (1991). This algorithm allows for mixture-averaged multi-component diffusion, thermal diffusion, variable thermochemical properties, and variable transport properties. The CHEMKIN package (Kee et al., 1992a, 1992b, 1993) was used as a preprocessor to find the thermochemical and transport properties for RUN-1DL. Transport properties were found from the transport property database of Kee et al. (1992b); thermochemical properties were found from the thermodynamic database of Kee et al. (1992a), except for HO_2 where the recommendations of Kim et al. (1994) were used. Before computing flame properties, all these properties were checked against original sources. Radiative heat losses were small (typically less than 0.4%) due to the large flame speeds of hydrogen-air flames and hence were neglected. Flame propagation was allowed to proceed sufficiently far (typically up to 30 mm) so that effects of initial conditions were small. Present measurements were limited

to flames having radii larger than 8 mm to avoid ignition disturbances, especially due to the stronger disturbances at higher pressures. Also, measurements were limited to the ratio of flame thickness to radius less than 2% so that effects of curvature and transient phenomena associated with large flame thicknesses were small. Finally, the computational grid in space and time was varied to ensure numerical accuracy within 1%. The flame position was taken at the point where gas temperatures were the average of the hot and cold boundaries. Due to stringent flame thickness limitations, however, the results were not affected significantly by the criterion used to define the flame position.

For the above conditions, the local (stretched) laminar burning velocity and flame stretch are given as follows (Strehlow and Savage, 1978):

$$S_L = (\rho_b/\rho_u) dr/dt, K = (2/r) dr/dt \quad (1)$$

where r , t and ρ_b/ρ_u are the flame radius, time and the density ratio of burned to unburned gases, respectively. The density ratio needed to find S_L from Eq. (1) was computed assuming adiabatic constant–pressure combustion with the same concentrations of elements in the unburned and burned gases. These calculations were carried out using the adiabatic equilibrium algorithm of Reynolds (1986). The computational results were analyzed to find flame/stretch interactions. At the aforementioned thin–flame limit conditions, the relationship between laminar burning velocity and flame stretch can be conveniently represented by combining an early proposal of Markstein (1964) and the “local conditions” hypothesis of Kwon et al. (1992), to yield:

$$S_{L\infty}/S_L = 1 + MaKa \quad (2)$$

where $S_{L\infty}$ is the unstretched downstream laminar burning velocity, Ma the Markstein number (representing the sensitivity of flame response to stretch) and Ka the Karlovitz number (the normalized flame stretch), which is defined as KD_u/S_L^2 where D_u is the binary mass diffusivity of hydrogen into the diluent (nitrogen). The small stretch limit is also of interest, to connect present results at finite levels of stretch to classical

asymptotic theories of laminar premixed flame propagation, as follows (Kwon and Faeth, 2001):

$$S_L/S_{L\infty} = 1 - Ma_\infty Ka_\infty, Ka_\infty \ll 1 \quad (3)$$

Fortuitously, both existing measurements and numerical simulations at normal temperature and normal to moderately elevated pressures yield a linear correlation between $S_{L\infty}/S_L$ and Ka , for values of Ka not too near quenching conditions, which implies constant Markstein numbers for each reactant condition (Kwon et al., 1992; Aung et al., 1998, 2002; Hassan et al., 1998; Kwon et al., 2000; Kwon and Faeth, 2001). In view of the complexity of laminar premixed flames a general proof of this constant Markstein number property is unlikely, however, once established for given conditions this behavior provides a very concise and helpful way of summarizing preferential-diffusion/stretch interactions. Thus, it is of major interest to explore the linear correlation at the present high temperature and pressure conditions.

Numerical simulations were conducted for hydrogen–air flames of fuel–equivalence ratio $\phi = 0.6$, which was a typical condition chosen through trade-offs among thermal efficiency, emission and power of hydrogen–fueled internal engines (McLean et al., 1977; Poulton, 1994), at pressures of 5 to 50 atm and temperatures of 500 to 1000 K, which were chosen based on James (1987), Abraham et al. (1985) and Gauducheau et al. (1998). In addition to these engine–like practical conditions, a simulation for the 5 atm and 298 K hydrogen–air flame was conducted as a reference data though this condition was out of the engine–like conditions. The test conditions and major results (which will be discussed later) are summarized in Table 1. All the calculations were carried out with the detailed hydrogen oxidation mechanism by Mueller et al. (1999), involving 9 species and 19 reversible reactions. This reaction mechanism was chosen based on a previous investigation (Kwon and Faeth, 2001) which showed good agreement between predicted and measured unstretched laminar burning velocities and Markstein numbers using the reaction mechanism for various conditions (including even various diluents).

Table 1 Summary of test conditions for hydrogen-air flames at high temperatures and pressures^a

p (atm)	T (K)	ρ_u/ρ_b (-)	D_u (mm ² /s)	$S_{L\infty}$ (mm/s)	Ka_{max} (-)	Ma (-)
$\phi=0.6$						
5 ^b	298	5.57	14.6	450	0.033	-4.8
5	500	3.61	35.6	1,610	0.015	-2.5
5	750	2.65	70.7	5,710	0.007	-0.1
5	1000	2.17	112.7	16,380	0.003	4.4
30	500	3.62	5.9	540	0.008	-4.8
30	750	2.66	11.7	2,220	0.003	-2.9
30	1000	2.18	18.8	7,650	0.001	-0.9
50	500	3.62	3.6	360	0.006	-5.1
50	750	2.66	7.0	1,530	0.002	-3.6
50	1000	2.18	11.3	5,310	0.001	0.0

^a Computations based on Mueller et al. (1999) mechanism.

^b A reference data at normal temperature; this condition is out of engine-like practical conditions.

3. Results and Discussion

3.1 Burning velocity/stretch interactions

Results for finite flame radii involve finite values of flame stretch so that the laminar burning velocity at the largest r computed, $S'_{L\infty}$, still differs from the fundamental unstretched laminar burning velocity of a plane flame, $S_{L\infty}$. Thus, values of $S_{L\infty}$ were found from Eq. (2) by plotting $S'_{L\infty}/S_L$ as a function of Ka . This yielded linear plots so that extrapolation to $Ka=0$ gave $S'_{L\infty}/S_L$ and thus $S_{L\infty}$, as summarized in Table 1 for the computations. Then given $S_{L\infty}$, plots of $S_{L\infty}/S_L$ as a function of Ka could be constructed for a given reactant mixture, pressure and temperature, as suggested by Eq. (2). Typical plots of this type are illustrated in Figs. 1 and 2 for hydrogen-air flames at 5 and 50 atm, respectively. The plot for 30 atm flames is not illustrated due to the very similar behavior to the 50 atm flames; results for the 30 atm flames are summarized in Table 1. Results at conditions that are stable (unstable) with respect to preferential-diffusion effects, corresponding to $Ma > 0$ ($Ma < 0$) and decreasing (increasing) burning velocities with increasing stretch, are indicated by open (darkened) symbols on these plots.

Results of simulations illustrated in Figs. 1 and 2 exhibit the linear relationship between $S_{L\infty}/S_L$

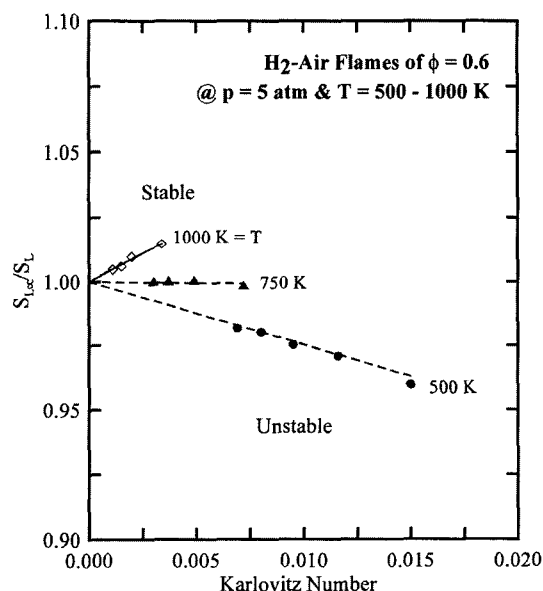


Fig. 1 Laminar burning velocities as a function of Karlovitz number and temperature for $\phi=0.6$ hydrogen-air flames at 5 atm

and Ka that was exploited to find $S_{L\infty}$ well within computational uncertainties; similar behavior was observed during earlier work for normal temperature and normal to moderately elevated pressures (Aung et al., 1998; Kwon and Faeth, 2001). Thus, the slope of each plot, which is equal to the Markstein number according to Eq. (2), is independent of Ka over the range of

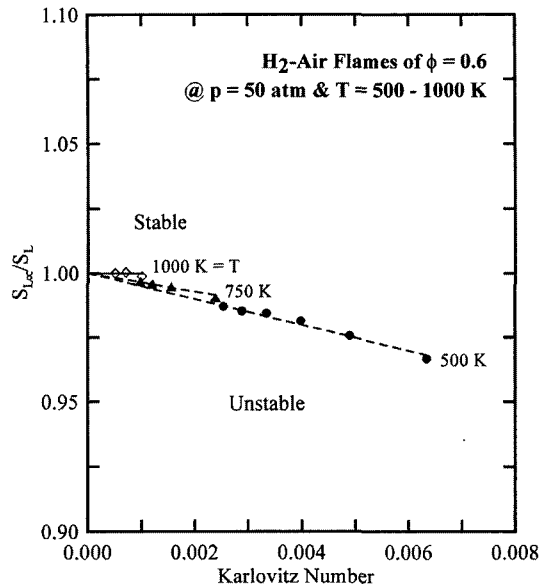


Fig. 2 Laminar burning velocities as a function of Karlovitz number and temperature for $\phi=0.6$ hydrogen–air flames at 50 atm

the computations on these figures (which involves $Ka < 0.015$). Similar behavior was observed over the entire test range, which involves $Ka < 0.033$. This observation indicates that the local conditions hypothesis is still valid for the present high temperature and pressure test conditions, and thus can be extended to the conditions in practical applications such as internal combustion engines. However, quenching effects as extinction conditions are approached (where Ka would be on the order of unity, see Law (1988)) would probably yield a more complex response to stretch.

For the present small values of Ka , effects of flame stretch on S_L were not significant: over the entire test range, $S_{L\infty}/S_L$ varied in the range of 0.95–1.02. Considering that the present tests were conducted for $Ka < 0.033$, which is much smaller than a typical value of 0.15 for hydrogen–fueled flames at normal temperature and pressure (Kwon and Faeth, 2001), however, the variation of $S_{L\infty}/S_L$ could be significant at moderate levels of stretch that are still far from the extinction conditions. For example, according to Keck (1982), Abraham et al. (1985) and Thomas

(1983), stretch \bar{K} can be estimated to be 2000 s^{-1} for a typical engine condition: the engine speed as a characteristic velocity scale, $V_c = 100 \text{ m/s}$ and the inlet valve diameter as a characteristic length scale, $L_c = 0.05 \text{ m}$. For this stretch level, the present relationship between $S_{L\infty}/S_L$ and Ka yields that the burning velocity can be changed up to 28% ($S_{L\infty} = 360 \text{ mm/s}$ and $S_L = 502 \text{ mm/s}$).

As discussed earlier, a linear variation of $S_{L\infty}/S_L$ with increasing Ka yields a constant Markstein number for each flame condition over the present test range. The properties of preferential-diffusion/stretch interactions are seen most concisely from the Markstein numbers, which are considered next.

3.2 Markstein numbers

Markstein numbers are independent of Karlovitz numbers for present conditions and are summarized in Table 1 as a function of reactant conditions. Predicted values of Ma for $\phi=0.6$ H_2 -air flames are plotted as a function of pressure in Fig. 3. Significant reductions of Ma with increasing pressure are observed in the figure. In particular, Ma for $T=1000 \text{ K}$ become zero and negative from a positive value at $p=5 \text{ atm}$ with increasing pressure, which enhances flame sensitivity to preferential-diffusion/stretch instability. It is very similar to past observations for hydrocarbon–air flames at normal temperature and normal to moderately elevated pressures (Hassan et al., 1998; Kwon et al., 2000) whereas this observation is somewhat different from that for hydrogen–fueled flames at normal temperature and sub-atmospheric to moderately elevated pressures (Aung et al., 1998; Kwon and Faeth, 2001) that exhibit a small effect of pressure on Ma (though still the same tendency, decreasing Ma with increasing pressure, was observed for the lean hydrogen flames). Considering all the above observations, however, the behavior of decreasing Ma with increasing pressure seems to be general, at least, for both hydrogen- and hydrocarbon-fueled flames at the high temperature and pressure conditions in the practical applications such as internal combustion engines. The increased sensitivity for unstable behavior appears to be

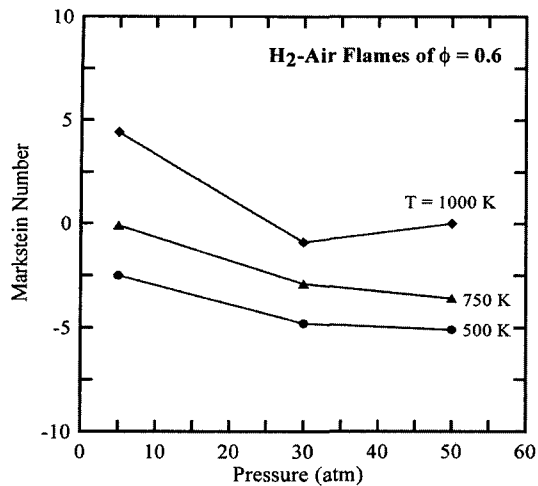


Fig. 3 Markstein numbers as a function of pressure for $\phi=0.6$ hydrogen-air flames at $T=500$, 750 and 1000 K

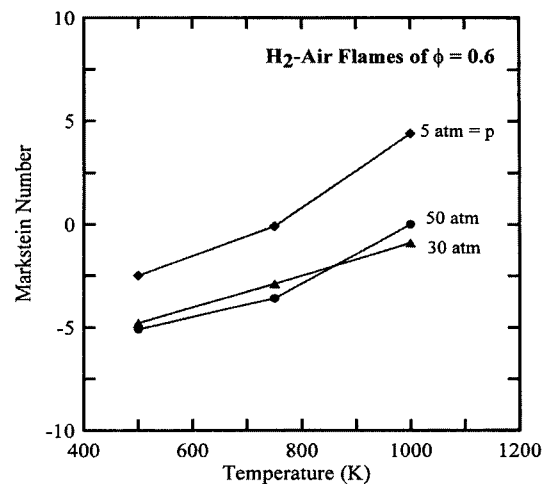


Fig. 4 Markstein numbers as a function of temperature for $\phi=0.6$ hydrogen-air flames at $p=5$, 30 and 50 atm

caused by reduced radical concentrations in the reaction zone and by reduced positive-stretch-generated stabilizing effects and enhanced baroclinic-torque-generated destabilizing effects due to reduced flame thicknesses (Kwon et al., 2000; Kwon and Faeth, 2001; Kwon et al., 2002).

In order to investigate the effects of initial mixture temperature on preferential-diffusion/stretch interactions at the high temperature conditions, Markstein numbers for $\phi=0.6$ H₂-air flames are plotted as a function of temperature in Fig. 4. In contrast to the pressure effects, Ma progressively increase with increasing temperature, which reduces flame sensitivity to preferential-diffusion/stretch instability. This observation is very similar to that for hydrogen-fueled flames at normal temperature and pressure (Kwon and Faeth, 2001). However, the observed general behavior of progressively increasing Ma with increasing temperature is somewhat different from an earlier experimental observation for heavy hydrocarbon-oxygen-nitrogen flames through an indirect method increasing flame temperature by increasing oxygen concentrations (Kwon et al., 2000), for which the Markstein numbers asymptotically approach $Ma=0$ with increasing temperature. Considering that the indirect method to increase flame temperature is actually different

from the present method to increase the temperature of the whole mixture field, however, the different behaviors were somewhat expected. For example, the present method yields significantly enhanced binary mass (and thermal) diffusivities of hydrogen into the mixture than those for the indirect method; the different values of transport parameters may affect positive-stretch-generated stabilizing effects and baroclinic-torque-generated destabilizing effects on the preferential-diffusion/stretch interactions.

Finally, the results in Figs. 3 and 4 suggest that though it depends on a specific condition whether the opposing effects of increased temperatures and increased pressures enhance or retard the instability of practical flames due to preferential-diffusion/stretch interactions compared to laboratory experiments at normal temperature and normal to moderately elevated pressure, the stabilizing effect due to increased temperatures is generally more dominant for the present test range ($T=298\sim 1000$ K and $p=5\sim 50$ atm). For example, compared to $Ma=-4.8$ for the flame at normal temperature and $p=5$ atm (Table 1), $Ma=4.4$ and -5.1 for $T=1000$ K and $p=5$ atm (max. T and min. p), and $T=500$ K and $p=50$ atm (min. T and max. p) flames respectively, which shows that the former stabilizing effect due

to T dominates the latter destabilizing effect due to p .

3.3 Unstretched laminar burning velocities

Effects of pressure on unstretched laminar burning velocities are summarized in Table 1 and are illustrated in Fig. 5. As discussed earlier, there was a linear relationship between $S_{L\infty}/S_L$ and Ka so that linear extrapolation to $Ka=0$ gave $S_{L\infty}$. Similar to the observations for hydrocarbon–air flames at normal temperature and normal to moderately elevated pressures (Hassan et al., 1998; Kwon et al., 2000), the figure shows a progressive reduction of $S_{L\infty}$ with the increasing flame pressure due to increased rates of three-body recombination reactions. However, this observation is somewhat different from the small pressure dependence of $S_{L\infty}$ for the hydrogen–air flames at normal temperature and sub-atmospheric to moderately elevated pressures (Aung et al., 1998). Based on numerical simulations at various fuel–equivalence ratios and pressures for laminar premixed hydrogen–air flames, Sun et al. (1999) showed that the pressure dependence of $S_{L\infty}$ for these hydrogen–fueled flames is somewhat complicated, e.g. the pressure exponent depends on the mixture compositions as well as the pressure range; therefore, it is difficult to find a general relationship between laminar burning velocities and pressure over a wide range of pressures (covering from sub-atmospheric to high pressures).

Effects of initial mixture temperature on unstretched laminar burning velocities are summarized in Table 1 and are illustrated in Fig. 6. Similar to the observations for heavy hydrocarbon–air and hydrogen–oxygen–diluent (argon or helium) flames at atmospheric conditions (Kwon et al., 2000; Kwon and Faeth, 2001), increasing the mixture temperatures yields a corresponding increase of $S_{L\infty}$. This behavior follows because increased flame temperatures at a fixed pressure tend to increase radical concentrations in the reaction zone of the flame. Then, based on the proportionality between radical concentrations in the reaction zone and laminar burning velocities (Kwon and Faeth, 2001), laminar burning

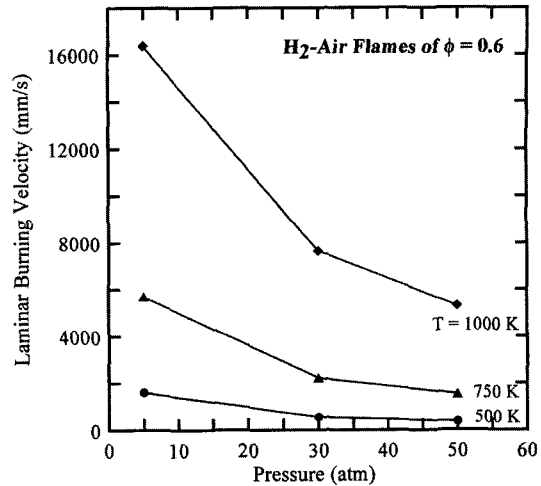


Fig. 5 Unstretched laminar burning velocities as a function of pressure for $\phi=0.6$ hydrogen–air flames at $T=500, 750$ and 1000 K

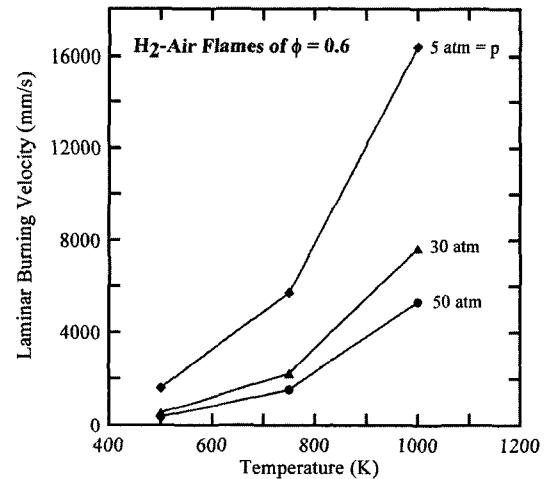


Fig. 6 Unstretched laminar burning velocities as a function of temperature for $\phi=0.6$ hydrogen–air flames at $p=5, 30$ and 50 atm

velocities increase accordingly.

4. Conclusions

Dynamic properties (preferential-diffusion/stretch interactions) of hydrogen–air flames were studied computationally. Outwardly propagating spherical premixed flames were considered for a fuel–equivalence ratio of 0.6, pressures of 5 to 50 atm, and temperatures of 298 to 1000 K in

order to understand the dynamic properties at conditions encountered in practical applications such as internal combustion engines. The major conclusions of the study are as follows :

(1) Effects of flame/stretch interactions for predictions could be correlated based on the local conditions hypothesis according to $S_{L\infty}/S_L=1+MaKa$ to obtain a linear relationship between $S_{L\infty}/S_L$ and Ka , yielding constant Markstein numbers for given reactant conditions, implying that the local conditions hypothesis can be extended to the practical conditions.

(2) Effects of flame stretch on laminar burning velocities were substantial, yielding the burning velocity changed up to 28% from the unstretched value for a typical engine condition ; the corresponding Ma was -5.1 .

(3) Opposing effects of increased temperatures and increased pressures on the instability of practical flames due to preferential-diffusion/stretch interactions were observed : increasing Ma with increasing T , while decreasing Ma with increasing p . Compared to laboratory experiments at normal temperature and normal to moderately elevated pressure, however, the stabilizing effects due to increased temperature are generally more dominant for the present test range.

(4) Unstretched laminar burning velocities increased with increasing temperatures and decreasing pressures.

Acknowledgment

This research was supported by Faculty Research Fund, Sungkyunkwan University, 2003.

References

Abraham, J., Williams, F. A. and Bracco, F. V., 1985, "A Discussion of Turbulent Flame Structure in Premixed Charges," *SAE* paper No. 850345.

Aung, K. T., Hassan, M. I. and Faeth, G. M., 1998, "Effects of Pressure and Nitrogen Dilution on Flame/Stretch Interactions of Laminar Premixed $H_2/O_2/N_2$ Flames," *Combustion and*

Flame, Vol. 112, pp. 1~15.

Aung, K. T., Hassan, M. I., Kwon, S., Tseng, L. -K., Kwon, O. C. and Faeth, G. M., 2002, "Flame/Stretch Interactions in Laminar and Turbulent Premixed Flames," *Combustion Science and Technology*, Vol. 174, pp. 61~99.

Bell, S. R. and Gupta, M., 1997, "Extension of the Lean Operating Limit for Natural Gas Fueling of a Spark Ignited Engine Using Hydrogen Blending," *Combustion Science and Technology*, Vol. 123, pp. 23~48.

Bradley, D., Hicks, R. A., Lawes, M., Sheppard, C. G. W. and Woolley, R., 1998, "The Measurement of Laminar Burning Velocities and Markstein Numbers for Iso-Octane-Air and Iso-Octane-n-Heptane in Air Mixtures at Elevated Temperatures and Pressures in an Explosion Bomb," *Combustion and Flame*, Vol. 115, pp. 126~144.

Clavin, P., 1985, "Dynamic Behavior of Premixed Flame Fronts in Laminar and Turbulent Flows," *Progress in Energy and Combustion Science*, Vol. 11, pp. 1~59.

DeLuchi, M. A., 1989, "Hydrogen Vehicles : An Evaluation of Fuel Storage, Performance, Safety, Environmental Impacts, and Cost," *International Journal of Hydrogen Energy*, Vol. 14, pp. 81~130.

Dowdy, D. R., Smith, D. B., Taylor, S. C. and Williams, A., 1990, "The Use of Expanding Spherical Flames to Determine Burning Velocities and Stretch Effects on Hydrogen/Air Mixtures," *Proceedings of the Combustion Institute*, Vol. 23, pp. 325~333.

Gauducheau, J. L., Denet, B. and Searby, G., 1998, "A Numerical Study of Lean CH_4/H_2 /Air Premixed Flames at High Pressure," *Combustion Science and Technology*, Vol. 137, pp. 81~99.

Hassan, M. I., Aung, K. T., Kwon, O. C. and Faeth, G. M., 1998, "Properties of Laminar Premixed Hydrocarbon/Air Flames at Various Pressures," *Journal of Propulsion and Power*, Vol. 14, pp. 479~488.

James, E. H., 1987, "Laminar Burning Velocities of Iso-Octane-Air Mixtures — A Literature Review," *SAE* paper No. 870170.

Keck, J. C., 1982, "Turbulent Flame Struc-

- ture and Speed in Spark-Ignition Engines," *Proceedings of the Combustion Institute*, Vol. 19, pp. 1451~1466.
- Kee, R. J., Rupley, F. M. and Miller, J. A., 1992a, "The CHEMKIN Thermodynamic Data Base," Report No. SAND87-8215B, Sandia National Laboratories, Albuquerque, NM.
- Kee, R. J., Dixon-Lewis, G., Warnatz, J., Coltrin, M. E. and Miller, J. A., 1992b, "A FORTRAN Computer Code Package for the Evaluation of Gas-Phase, Multi-Component Transport Properties," Report No. SAND86-8246, Sandia National Laboratories, Albuquerque, NM.
- Kee, R. J., Rupley, F. M. and Miller, J. A., 1993, "CHEMKIN II: A Fortran Chemical Kinetics Package for the Analysis of Gas Phase Chemical Kinetics," Report No. SAND89-8009B, Sandia National Laboratories, Albuquerque, NM.
- Kim, T. J., Yetter, R. A. and Dryer, F. L., 1994, "New Results on Moist CO Oxidation: High Pressure, High Temperature Experiments and Comprehensive Kinetic Modeling," *Proceedings of the Combustion Institute*, Vol. 25, pp. 759~766.
- Kwon, O. C., Hassan, M. I. and Faeth, G. M., 2000, "Flame/Stretch Interactions of Premixed Fuel-Vapor/O₂/N₂ Flames," *Journal of Propulsion and Power*, Vol. 16, pp. 513~522.
- Kwon, O. C. and Faeth, G. M., 2001, "Flame/Stretch Interactions of Premixed Hydrogen-Fueled Flames: Measurements and Predictions," *Combustion and Flame*, Vol. 124, pp. 590~610.
- Kwon, O. C., Rozenchan, G. and Law, C. K., 2002, "Cellular Instabilities and Self-Acceleration of Outwardly Propagating Spherical Flames," *Proceedings of the Combustion Institute*, Vol. 29, pp. 1775~1783.
- Kwon, S., Tseng, L.-K. and Faeth, G. M., 1992, "Laminar Burning Velocities and Transition to Unstable Flames in H₂/O₂/N₂ and C₃H₈/O₂/N₂ Mixtures," *Combustion and Flame*, Vol. 90, pp. 230~246.
- Kyaw, Z. H. and Watson, H. C., 1992, "Hydrogen Assisted Jet Ignition for Near Elimination of NO_x and Cyclic Variability in the S. I. Engine," *Proceedings of the Combustion Institute*, Vol. 24, pp. 1449~1455.
- Law, C. K., 1988, "Dynamics of Stretched Flames," *Proceedings of the Combustion Institute*, Vol. 22, pp. 1381~1402.
- McLean, W. J., de Boer, P. C. T., Homan, H. S. and Fagelson, J. J., 1977, "Hydrogen as a Reciprocating Engine Fuel," Future Automotive Fuels (J. M. Colucci and N. E. Gallopoulos, Eds.), Plenum press, New York, pp. 297~319.
- Markstein, G. H., 1964, *Non-Steady Flame Propagation*, Pergamon, New York, p. 22.
- Mathur, H. B., Das, L. M. and Patro, T. N., 1992, "Hydrogen Fuel Utilization in CI Engine Powered End Utility Systems," *International Journal of Hydrogen Energy*, Vol. 17, pp. 369~374.
- Mueller, M. A., Kim, T. J., Yetter, R. A. and Dryer, F. L., 1999, "Flow Reactor Studies and Kinetic Modeling of the H₂/O₂ Reaction," *International Journal of Chemical Kinetics*, Vol. 31, pp. 113~125.
- Ogden, J. M., 1999, "Developing an Infrastructure for Hydrogen Vehicles: A Southern California Case Study," *International Journal of Hydrogen Energy*, Vol. 24, pp. 709~730.
- Poulton, M. L., 1994, *Alternative Fuels for Road Vehicles*, Computational Mechanics, Southampton, UK, pp. 157~167.
- Reynolds, W. C., 1986, "The Element Potential Method for Chemical Equilibrium Analysis: Implementation in the Interactive Program STANJAN," Department of Mechanical Engineering Report, Stanford University, Stanford, CA.
- Rogg, B., 1991, "RUN-1DL: The Cambridge Universal Laminar Flame Code," Technical Report CUED/A-THERMO/TR39, Department of Engineering, University of Cambridge, Cambridge, UK.
- Strehlow, R. A. and Savage, L. D., 1978, "The Concept of Flame Stretch," *Combustion and Flame*, Vol. 31, pp. 209~211.
- Sun, C. J., Sung, C. J., He, L. and Law, C. K., 1999, "Dynamics of Weakly Stretched Flames: Quantitative Description and Extraction of Global Flame Parameters," *Combustion and Flame*, Vol. 118, pp. 108~128.
- Thomas, A., 1983, "Flame Development in

Spark-Ignition Engines," *Combustion and Flame*, Vol. 50, pp. 305~322.

Verhelst, S. and Sierens, R., 2001, "Aspects Concerning the Optimization of a Hydrogen Fueled Engine," *International Journal of Hydrogen Energy*, Vol. 26, pp. 981~985.

Yamaoka, I. and Tsuji, H., 1992, "An Anomalous Behavior of Methane-Air and Methane-Hy-

drogen-Air Flames Diluted with Nitrogen in a Stagnation Flow," *Proceedings of the Combustion Institute*, Vol. 24, pp. 145~152.

Yu, G., Law, C. K. and Wu, C. K., 1986, "Laminar Flame Speeds of Hydrocarbon + Air Mixtures with Hydrogen Addition," *Combustion and Flame*, Vol. 63, pp. 339~347.